

Synthesis and Characterization of Ferroelectric Liquid Crystalline Polysiloxanes and Polymethacrylates Containing [(S)-2-Methyl-1-butoxy]phenyl 4-(Alkyloxy)biphenyl-4'-carboxylate Side Groups

Chain-Shu Hsu,* Jhy-Horung Lin, and Ling-Rong Chou

Department of Applied Chemistry, National Chiao Tung University, Hsinchu, Taiwan 30050, ROC

Ging-Ho Hsiue

Department of Chemical Engineering, National Tsing Hua University, Hsinchu, Taiwan 30049, ROC

Received May 18, 1992; Revised Manuscript Received September 8, 1992

ABSTRACT: The synthesis of side-chain liquid crystalline polysiloxanes and polymethacrylates containing 4-[(S)-2-methyl-1-butoxy]phenyl 4-hydroxybiphenyl-4'-carboxylate moieties as mesogenic units and aliphatic spacers containing respectively three to eleven methylene units is presented. Differential scanning calorimetry, optical polarizing microscopy, and X-ray diffraction measurements reveal chiral smectic mesomorphism for all polymers. Both polysiloxanes which contain respectively six and eleven methylene units in the spacers exhibit smectic A, chiral smectic C, and smectic B phases. Among the polymethacrylates prepared in this study, the polymethacrylate containing eleven methylene units in its spacers is the only one revealing smectic A and chiral smectic C phases. The results seem to demonstrate that the tendency toward chiral smectic C mesomorphism increases with increasing spacer length, and the thermal stability of the chiral smectic C mesophase is determined by the flexibility of the polymer backbone.

Introduction

In 1975 Mayer¹ presented theoretically and then proved experimentally that the chiral smectic C (S_C^{*}) mesophase was ferroelectric. A bistable, fast switching, electrooptical device which uses the ferroelectric liquid crystals (FLCs) was demonstrated a few years later by Clark and Lagerwell.² An increasing interest in the synthesis of low molar mass S_C^{*} liquid crystals has since then developed. Numerous FLC compounds and room-temperature mixtures have so far been prepared for fast electrooptical applications.

Besides low molar mass FLCs, several side-chain liquid crystalline polymers (LCPs) exhibiting a S_C^{*} mesophase have recently been reported.³⁻²⁶ Ferroelectric properties, e.g. spontaneous polarization in these polymers, have also been provided in some cases.^{1,12,16-25} This field has been reviewed by LeBarny and Dubois.²⁷ The detailed structure-property relationship of S_C^{*} LCPs, however, has not been very clear up until now. This has been due to the limited experimental data reported in the literature.

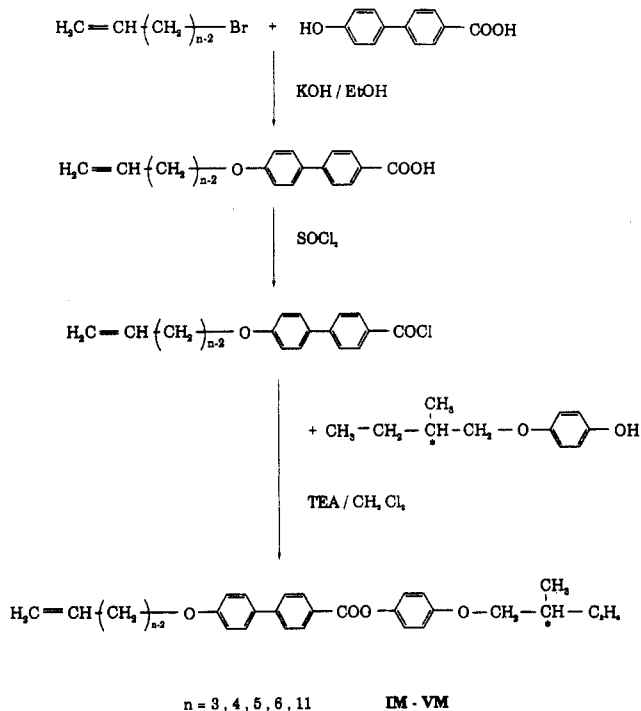
Presenting the synthesis of some chiral smectic liquid crystalline polysiloxanes and polymethacrylates containing 4-[(S)-2-methyl-1-butoxy]phenyl 4-(alkyloxy)biphenyl-4'-carboxylate side groups is the goal of this study. Their characterizations by differential scanning calorimetry, optical polarizing microscopy, and X-ray diffraction have been presented.

Experimental Section

A. Materials. Poly(methylhydrosiloxane) ($\bar{M}_n = 2270$) and divinyltetramethyldisiloxane platinum catalyst were obtained from Patrarch System Inc. and used as received. (S)-(-)-2-Methyl-1-butanol, $[\alpha]_D^{25} = -6.5^\circ$ (from Merck), 4-hydroxybiphenyl-4'-carboxylate (from Tokyo Kasei Co.), and all other reagents (from Aldrich) were used as received. Toluene used in the hydrosilation reaction and 1,3-dioxane were first refluxed

* To whom all correspondence should be addressed.

Scheme I Synthesis of Monomers IM-VM



over sodium and then distilled under nitrogen. 2,2'-Azobisisobutyronitrile (AIBN) (from Fluka) was freshly recrystallized from methanol.

B. Techniques. ¹H NMR spectra (300 MHz) were recorded on a Varian VXR-300 spectrometer. FT-IR spectra were measured on a Nicolet 520 FT-IR spectrometer. Polymer samples were cast as films on a KBr tablet for the measurement. Thermal transitions and thermodynamic parameters were determined by using a Seiko SSC/5200 differential scanning calorimeter equipped with a liquid nitrogen cooling accessory. Heating and cooling rates were 10 °C/min. Thermal transitions reported were collected during the second heating and cooling scans. A Nikon

Table I
Characterization of Monomers IM-VM

monomer	yield, %	$[\alpha]^{25}_D$	400-MHz ^1H NMR (CDCl_3 , δ , ppm)
IM	77	+4.087	0.88 (t, 3 H, $-\text{CH}_2-\text{CH}_3$), 0.96 [d, 3 H, $-\text{CH}(\text{CH}_3)-$], 1.21-1.52 (m, 2 H, $-\text{CH}_2-\text{CH}_3$), 1.86 [m, 1 H, $-\text{CH}(\text{CH}_3)-$], 3.72 [m, 2 H, $-\text{OCH}_2-\text{CH}(\text{CH}_3)-$], 4.54 (d, 2 H, $-\text{CH}_2-\text{OPh}$), 5.03 (m, 2 H, $\text{CH}_2=$), 5.80 (m, 1 H, $=\text{CH}-$), 6.86-8.17 (m, 12 aromatic protons)
IIM	74	+4.553	0.88 (t, 3 H, $-\text{CH}_2-\text{CH}_3$), 0.96 [t, 3 H, $-\text{CH}(\text{CH}_3)-$], 1.19-1.53 (m, 2 H, $-\text{CH}_2-\text{CH}_3$), 1.80 [m, 1 H, $-\text{CH}(\text{CH}_3)-$], 2.52 (m, 2 H, $-\text{CH}_2-\text{CH}=\text{CH}_2$), 3.73 [m, 2 H, $-\text{OCH}_2-\text{CH}(\text{CH}_3)-$], 4.01 (t, 2 H, $-\text{CH}_2-\text{OPh}$), 5.10 (m, 2 H, $\text{CH}_2=$), 5.88 (m, 1 H, $=\text{CH}-$), 6.86-8.17 (m, 12 aromatic protons)
IIIM	75	+4.470	0.88 (t, 3 H, $-\text{CH}_2-\text{CH}_3$), 0.96 [t, 3 H, $-\text{CH}(\text{CH}_3)-$], 1.17-1.89 [m, 5 H, $-\text{CH}_2-$ and $-\text{CH}(\text{CH}_3)-\text{CH}_2-$], 2.20 (m, 2 H, $-\text{CH}_2-\text{CH}=\text{CH}_2$), 3.72 [m, 2 H, $-\text{OCH}_2-\text{CH}(\text{CH}_3)-$], 3.97 (t, 2 H, $-\text{CH}_2-\text{OPh}$), 4.99 (m, 2 H, $\text{CH}_2=$), 5.81 (m, 1 H, $=\text{CH}-$), 6.86-8.17 (m, 12 aromatic protons)
IVM	71	+4.967	0.88 (t, 3 H, $-\text{CH}_2-\text{CH}_3$), 0.95 [d, 3 H, $-\text{CH}(\text{CH}_3)-$], 1.14-1.81 [m, 7 H, $(-\text{CH}_2)_2$ and $-\text{CH}(\text{CH}_3)-\text{CH}_2-$], 2.07 (m, 2 H, $-\text{CH}_2-\text{CH}=\text{CH}_2$), 3.72 [m, 2 H, $-\text{OCH}_2-\text{CH}(\text{CH}_3)-$], 3.81 (t, 2 H, $-\text{CH}_2-\text{OPh}$), 5.10 (m, 2 H, $\text{CH}_2=$), 5.86 (m, 1 H, $=\text{CH}-$), 6.86-8.16 (m, 12 aromatic protons)
VM	43	+4.220	0.86 (t, 3 H, $-\text{CH}_2-\text{CH}_3$), 0.94 [d, 3 H, $-\text{CH}(\text{CH}_3)-$], 1.18-1.80 [m, 17 H, $(-\text{CH}_2)_7$ and $-\text{CH}(\text{CH}_3)-\text{CH}_2-$], 2.03 (m, 2 H, $-\text{CH}_2-\text{CH}=\text{CH}_2$), 3.91 [m, 2 H, $-\text{OCH}_2-\text{CH}(\text{CH}_3)-$], 4.11 (m, 2 H, $-\text{CH}_2-\text{OPh}$), 4.90 (m, 2 H, $\text{CH}_2=$), 5.76 (m, 1 H, $=\text{CH}-$), 6.90-8.14 (m, 12 aromatic protons)

Table II
Characterization of Compounds VIA-VIIIA

compd	yield, %	mp, $^\circ\text{C}$	400-MHz ^1H NMR (CDCl_3 , δ , ppm)
VIA	40	136.8	1.01 (t, 3 H, $-\text{CH}_2-\text{CH}_3$), 1.07 [d, 3 H, $-\text{CH}(\text{CH}_3)-$], 1.29-1.62 (m, 2 H, $-\text{CH}_2-\text{CH}_3$), 1.91 [m, 1 H, $-\text{CH}(\text{CH}_3)-$], 2.31 (m, 2 H, $-\text{CH}_2-$), 3.83 [m, 2 H, $-\text{O}-\text{CH}_2-\text{CH}(\text{CH}_3)-$], 3.95 (t, 2 H, $-\text{CH}_2\text{O}-\text{Ph}$), 4.24 (t, 2 H, $\text{HO}-\text{CH}_2-$), 6.97-8.28 (m, 12 aromatic protons)
VIIA	51	122.3	0.87 (t, 3 H, $-\text{CH}_2-\text{CH}_3$), 0.94 [d, 3 H, $-\text{CH}(\text{CH}_3)-$], 1.27-1.56 [m, 10 H, $-\text{CH}_2-\text{CH}_3$ and $(-\text{CH}_2)_4$], 1.74 [m, 1 H, $-\text{CH}(\text{CH}_3)-$], 3.58 (t, 2 H, $-\text{CH}_2-\text{OPh}$), 3.71 (m, 2 H, $-\text{OCH}_2-\text{CH}(\text{CH}_3)-$), 3.95 (t, 2 H, $\text{HO}-\text{CH}_2-$), 6.84-8.16 (m, 12 aromatic protons)
VIIIA	77	113.7	0.88 (t, 3 H, $-\text{CH}_2-\text{CH}_3$), 0.95 [d, 3 H, $-\text{CH}(\text{CH}_3)-$], 1.23-1.52 [m, 20 H, $-\text{CH}_2-\text{CH}_3$ and $(-\text{CH}_2)_9$], 1.74 [m, 1 H, $-\text{CH}(\text{CH}_3)-$], 3.56 (t, 2 H, $-\text{CH}_2-\text{OPh}$), 3.71 [m, 2 H, $-\text{OCH}_2-\text{CH}(\text{CH}_3)-$], 3.95 (t, 2 H, $\text{HO}-\text{CH}_2-$), 6.85-8.15 (m, 12 aromatic protons)

Table III
Characterization of Monomers VIM-VIIIM

monomer	yield, %	$[\alpha]^{25}_D$	400-MHz ^1H NMR (CDCl_3 , δ , ppm)
VIM	55	+5.10	0.86 (t, 3 H, $-\text{CH}_2-\text{CH}_3$), 1.01 [d, 3 H, $-\text{CH}(\text{CH}_3)-$], 1.21-1.90 [m, 3 H, $-\text{CH}(\text{CH}_3)-\text{CH}_2-$], 1.94 (s, 3 H, $=\text{C}-\text{CH}_3$), 2.20 (m, 2 H, $-\text{CH}_2-\text{CH}_2-\text{CH}_2\text{O}-$), 3.75 [m, 2 H, $-\text{OCH}_2-\text{CH}(\text{CH}_3)-$], 4.12 (t, 2 H, $-\text{CH}_2-\text{OPh}$), 4.35 (t, 2 H, $-\text{COO}-\text{CH}_2-$), 5.57 and 6.11 (2 d, 2 H, $\text{CH}_2=$), 6.92-8.23 (m, 12 aromatic protons)
VIIM	41	+3.12	0.88 (t, 3 H, $-\text{CH}_2-\text{CH}_3$), 0.98 [d, 3 H, $-\text{CH}(\text{CH}_3)-$], 1.22-1.83 [m, 11 H, $(-\text{CH}_2)_4$ and $-\text{CH}(\text{CH}_3)-\text{CH}_2-$], 1.87 (s, 3 H, $=\text{C}-\text{CH}_3$), 3.85 [m, 2 H, $-\text{OCH}_2-\text{CH}(\text{CH}_3)-$], 3.93 (t, 2 H, $-\text{CH}_2-\text{OPh}-$), 4.10 (t, 2 H, $-\text{COO}-\text{CH}_2-$), 5.47 and 6.02 (d, 2 H, $\text{CH}_2=$), 6.85-8.20 (m, 12 aromatic protons)
VIIIM	60	+4.55	0.93 (t, 3 H, $-\text{CH}_2-\text{CH}_3$), 0.99 [d, 3 H, $-\text{CH}(\text{CH}_3)-$], 1.21-1.83 [m, 21 H, $(-\text{CH}_2)_9$ and $-\text{CH}(\text{CH}_3)-\text{CH}_2-$], 1.91 (s, 3 H, $=\text{C}-\text{CH}_3$), 3.76 [m, 2 H, $-\text{OCH}_2-\text{CH}(\text{CH}_3)-$], 3.98 (t, 2 H, $-\text{CH}_2-\text{OPh}-$), 4.11 (t, 2 H, $-\text{COO}-\text{CH}_2-$), 5.51 and 6.07 (2 d, 2 H, $\text{CH}_2=$), 6.90-8.21 (m, 12 aromatic protons)

Microphot-FX optical polarized microscope equipped with a Mettler FP 82 hot stage and a FP 80 central processor was used to observe the thermal transitions and to analyze the anisotropic textures. Preparative gel permeation chromatography (GPC) was run on a Waters 510 LC instrument equipped with a 410 differential refractometer and a preparative GPC column (22.5 mm \times 60 cm) supplied by American Polymer Standard Co. X-ray diffraction measurements were performed with nickel-filtered $\text{Cu K}\alpha$ radiation with a Rigaku powder diffractometer. Optical rotations were measured at 25 $^\circ\text{C}$ on a Jasco DIP-140 polarimeter with chloroform as solvent for all compounds.

C. Synthesis of Monomers. The synthesis of olefin monomers IM-VM for the hydrosilation reaction and methacrylate monomers VIM-VIIIM is outlined in Schemes I and III. (S)-2-Methyl-1-butyl tosylate, 10-undecen-1-yl tosylate, 4-bromo-1-butene, 5-bromo-1-pentene, and 6-bromo-1-hexene were synthesized according to literature procedures.^{28,29} The optical rotation, $[\alpha]^{25}_D$ of (S)-2-methyl-1-butyl tosylate is +4.6 $^\circ$.

4-[(S)-2-Methyl-1-butoxy]phenyl Benzyl Ether. *p*-(Benzoyloxy)phenol (20.8 g, 0.104 mol) was added to a stirred solution of KOH (5.9 g, 0.104 mol) and KI (1.0 g) in 250 mL of 95% ethanol. (S)-2-Methyl-1-butyl tosylate (25.2 g, 0.104 mol) was added when dissolution was complete. The solution was refluxed for 3 h and cooled to room temperature. The solvent was then removed in a rotovap. The residue was washed with water and extracted with diethyl ether. The ether layer was dried over

anhydrous MgSO_4 , filtered, and evaporated to dryness. The crude product was recrystallized from methanol to yield 23.9 g (85%) of white crystals; mp = 33.6 $^\circ\text{C}$. ^1H NMR (CDCl_3 , δ , ppm): 0.90-1.01 (m, 6 H, CH_3-), 1.18-1.63 (m, 2 H, $-\text{CH}_2-$), 1.82 (m, 1 H, $>\text{CH}-$), 3.70 (m, 2 H, $-\text{CH}_2\text{OPh}$), 5.00 (s, 2 H, $\text{Ph}-\text{CH}_2-\text{OPh}$), 6.81-7.42 (m, 9 aromatic protons).

4-[(S)-2-Methyl-1-butoxy]phenol. Sodium (18.4 g, 0.80 mol) was added rapidly but in small pieces to a hot solution of 4-[(S)-2-methyl-1-butoxy]phenyl benzyl ether (21.6 g, 0.80 mol) in anhydrous *t*-BuOH (150 mL). The solution was heated to reflux for 20 h. A small amount of cold water was added after the sodium had all reacted. This was followed by the addition of a cold, dilute hydrochloric acid solution. The *t*-BuOH was removed in a rotovap, and the residue was extracted with diethyl ether. The collected diethyl ether solution was washed with water, dried over anhydrous MgSO_4 , and then evaporated to dryness. The obtained product was purified by column chromatography (silica gel, ethyl acetate/*n*-hexane = 1:10 as eluent) to yield 13.35 g (92.7%) of white crystals; mp = 45.6 $^\circ\text{C}$; $[\alpha]^{25}_D = -8.44^\circ$. ^1H NMR (CDCl_3 , δ , ppm): 0.89-0.98 (m, 6 H, CH_3-), 1.18-1.56 (m, 2 H, $-\text{CH}_2-$), 1.80 (m, 1 H, $>\text{CH}-$), 3.69 (m, 2 H, $-\text{CH}_2\text{OPh}$), 5.01 (s, 1 H, $-\text{OH}$), 6.71-6.77 (2d, 4 aromatic protons).

4-(Allyloxy)biphenyl-4'-carboxylic Acid, 4-(3-Buten-1-yloxy)biphenyl-4'-carboxylic Acid, 4-(4-Penten-1-yloxy)biphenyl-4'-carboxylic Acid, 4-(5-Hexen-1-yloxy)biphenyl-4'-carboxylic Acid, and 4-(10-Undecen-1-yloxy)biphenyl-

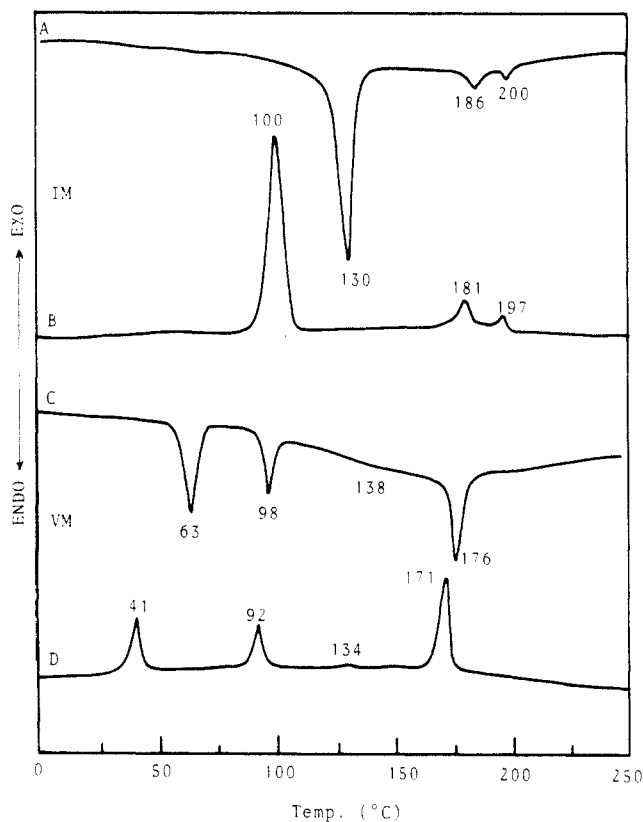


Figure 1. DSC thermogram (10 °C/min): (A) IM, second heating scan; (B) IM, cooling scan; (C) VM, second heating scan; (D) VM, cooling scan.

Table IV
Phase Transitions and Phase-Transition Enthalpies for Monomers IM-VM

monomer	n^a	phase transitions, °C (corresponding enthalpy changes, kcal/mol)	
		heating	cooling
IM	3	K 130 (3.89) S_A 186 (0.37) N* 200 (0.14) I	I 197 (0.11) N* 181 (0.38) S_A 100 (4.08) K
IIM	4	K 131 (4.56) S_A 187 N* 194 (0.84) I	I 193 (0.14) N* 191 (0.54) S_A 92 (3.79) K
IIIM	5	K 139 (5.98) S_A 183 (0.22) N* 200 (1.64) I	I 199 (0.67) N* 195 (0.67) S_A 101 (2.89) K
IVM	6	K 116 (5.25) S_A 193 (1.26) I	I 187 (1.48) S_A 109 (0.71) S_B 86.6 (0.66) K
VM	11	K 63 (0.93) S_B 98 (0.61) S_C^* 138 (-) ^b S_A 176 (1.56) I	I 171 (1.34) S_A 134 (-) ^b S_C^* 92 (0.61) S_B 41 (1.05) K

^a n according to Scheme I. ^b Enthalpy is very small.

4'-carboxylic Acid. All five compounds were prepared by the etherification of alkenyl bromides or undecenyl tosylate with 4-hydroxybiphenyl-4'-carboxylic acid. The synthesis of 4-(allyloxy)biphenyl-4'-carboxylic acid is described below.

4-Hydroxybiphenyl-4'-carboxylic acid (6 g, 0.028 mol) was added to a solution of KOH (3.76 g, 0.067 mol) and KI (0.2 g) in 90% ethanol (150 mL). The solution was refluxed for 1 h, and allyl bromide (4.56 g, 0.034 mol) was added dropwise. The resulting solution was refluxed for 20 h and cooled to room temperature, and 100 mL of water was added. The solution was acidified with dilute hydrochloric acid. The precipitate was filtered and recrystallized from acetic acid to yield 4.76 g (66.9%) of white crystals; mp = 232.9 °C. ¹H NMR (CDCl₃, δ , ppm): 4.60

Scheme II
Synthesis of Polysiloxanes IP-VP

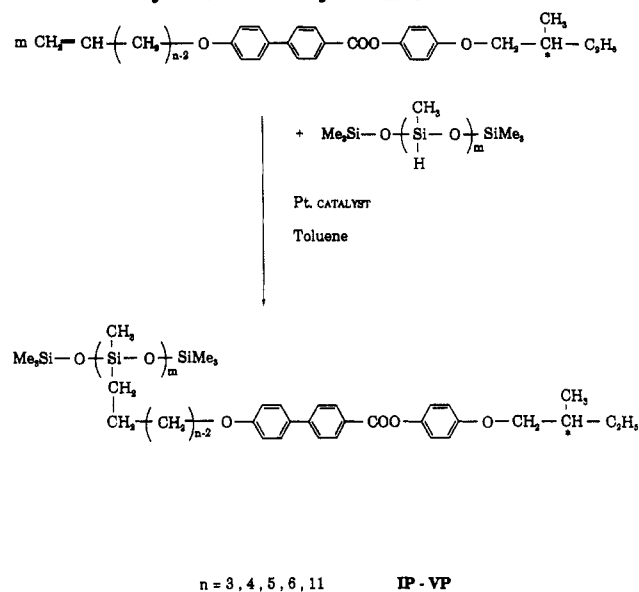


Table V
Thermal Transitions and Phase-Transition Enthalpies for Polymers IP-VP

polymer	n^a	phase transitions, °C (corresponding enthalpy change, kcal/mru ^b)	
		heating	cooling
IP	3	g 25 S_A 117 (1.82) I	I 99 (1.80) S_A
IIP	4	g 18 S_A 84 (0.78) I	I 80 (0.42) S_A
IIIP	5	g 22 S_B 99 (0.89) S_A 212 (0.86) I	I 204 (0.68) S_A 89 (0.82) S_B
IVP	6	g 16 S_B 120 (1.73) S_C^* 166 (-) ^c S_A 244 (1.24) I	I 236 (0.98) S_A 164 (-) ^c S_C^* 109 (1.47) S_B
VP	11	g 20 S_B 109 (0.78) S_C^* 143 (-) ^c S_A 218 (0.86) I	I 210 (0.89) S_A 142 (-) ^c S_C^* 103 (0.74) S_B

^a n according to Scheme II. ^b mru = mole repeating unit. ^c Enthalpy is very small.

(d, 2 H, -CH₂-), 5.40 (m, 2 H, CH₂=), 6.08 (m, 1 H, =CH-), 6.98-8.16 (m, 8 aromatic protons).

4-[(*S*)-2-Methyl-1-butoxy]phenyl 4-(Allyloxy)biphenyl-4'-carboxylate (IM), 4-[(*S*)-2-Methyl-1-butoxy]phenyl 4-(3-Buten-1-yloxy)biphenyl-4'-carboxylate (IIM), 4-[(*S*)-2-Methyl-1-butoxy]phenyl 4-(4-Penten-1-yloxy)biphenyl-4'-carboxylate (IIIM), 4-[(*S*)-2-Methyl-1-butoxy]phenyl 4-(5-Hexen-1-yloxy)biphenyl-4'-carboxylate (IVM), and 4-[(*S*)-2-Methyl-1-butoxy]phenyl 4-(10-Undecen-1-yloxy)biphenyl-4'-carboxylate (VM). All five olefin monomers (IM-VM) were prepared by the same method. The synthesis of monomer IM is described below.

4-(Allyloxy)biphenyl-4'-carboxylic acid (1.524 g, 0.006 mol) was reacted at room temperature with excess thionyl chloride (4 mL) containing a few drops of dimethylformamide in methylene chloride (7 mL) for 2 h. The solvent and excess thionyl chloride were removed under reduced pressure to give the corresponding acid chloride. The product was dissolved in 20 mL of methylene chloride and slowly added to a cold solution of 4-[(*S*)-2-methyl-1-butoxy]phenol (1.08 g, 0.006 mol) and triethylamine (1.67 mL) in 100 mL of methylene chloride. The solution was stirred at

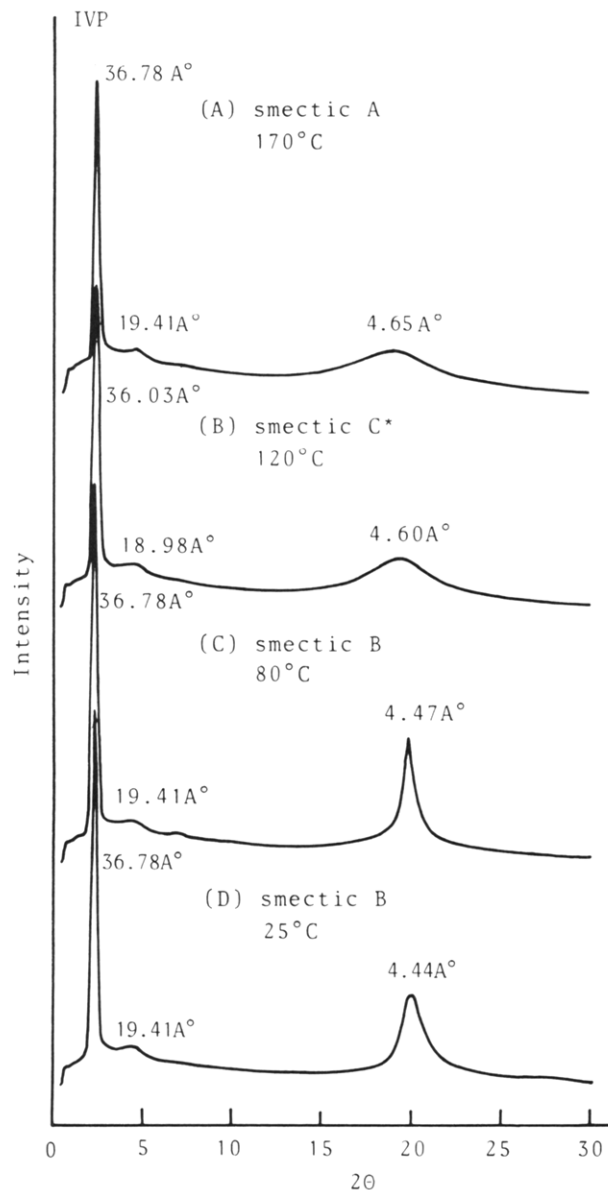


Figure 2. Temperature-dependent X-ray measurements for polymer IVP at (A) 170 °C, (B) 120 °C, (C) 80 °C, and (D) 25 °C.

room temperature. The solvent was then distilled. The obtained crude product was dissolved in methylene chloride and passed through silica gel. The solvent was removed in a rotovap. The product was recrystallized from a mixture of methanol and benzene to yield 1.93 g (77.2%) of white crystals. The yields, melting points, optical rotations, and ^1H NMR chemical shifts of all synthesized monomers have been summarized in Table I.

4-[(*S*)-2-Methyl-1-butoxy]phenyl 4-[(3-Hydroxyprop-1-yl)oxy]biphenyl-4'-carboxylate (VIA), 4-[(*S*)-2-Methyl-1-butoxy]phenyl 4-[(6-Hydroxyhex-1-yl)oxy]biphenyl-4'-carboxylate (VIIA), and 4-[(*S*)-2-Methyl-1-butoxy]phenyl 4-[(11-Hydroxyundec-1-yl)oxy]biphenyl-4'-carboxylate (VIII A). All three compounds were prepared by the same method. The synthesis of compound VIII A is described below.

Into a dry three-neck flask equipped with a thermometer, a pressure-equilibrated dropping funnel, and a reflux condenser fitted with a nitrogen adaptor and connected to a silicon oil bubbler was placed a solution of 4-[(*S*)-2-methyl-1-butoxy]phenyl 4-(10-undecen-1-yloxy)biphenyl-4'-carboxylate (1.32 g, 2.5 mmol) in dry THF (6 mL). 9-BBN (6 mL, 3.0 mmol), 0.5 M solution in THF, was charged via a syringe into the dropping funnel and then added dropwise into the stirring olefin solution. The mixture was oxidized after the addition was completed. A solution of 3 N NaOH (1 mL) was injected into the flask, followed by 3 mL of 30% H_2O_2 solution, which was added dropwise over 15 min.

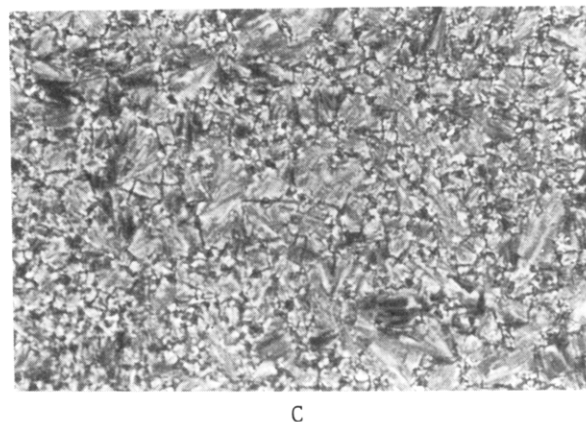
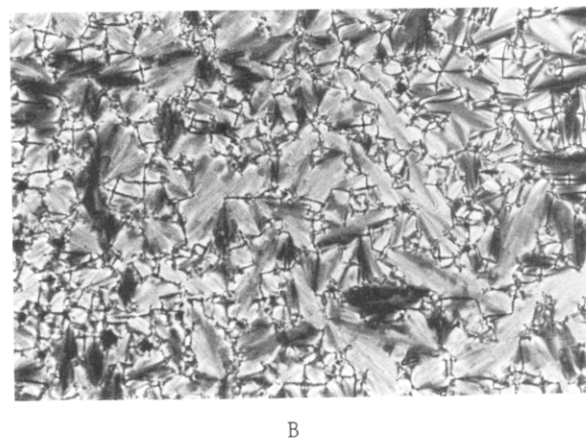
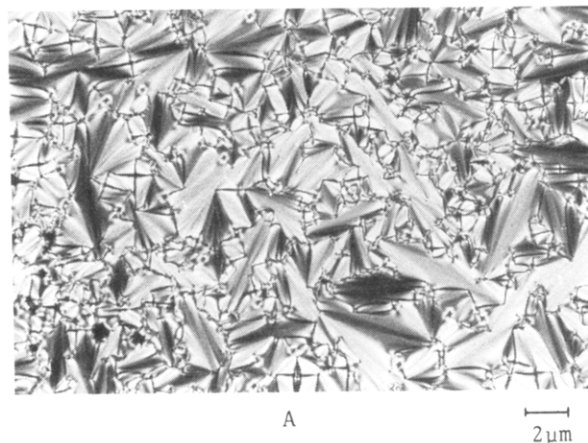


Figure 3. Optical polarizing micrographs displayed by IVP: (A) S_A texture obtained after cooling to 198.2 °C; (B) S_C^* texture obtained cooling to 161.8 °C; (C) S_B texture obtained after cooling to 98.0 °C.

The reaction mixture was stirred for 1 additional h and poured into water. The precipitated product was filtered, washed with water, dried, and finally recrystallized from toluene to yield 1.05 g (77%) of white crystals. The yields, melting points, and ^1H NMR chemical shifts of compounds VIA–VIII A are summarized in Table II.

4-[(*S*)-2-Methyl-1-butoxy]phenyl 4-[(3-Methacryloyl-prop-1-yl)oxy]biphenyl-4'-carboxylate (VIM), 4-[(*S*)-2-Methyl-1-butoxy]phenyl 4-[(6-Methacryloylhex-1-yl)oxy]biphenyl-4'-carboxylate (VIIM), and 4-[(*S*)-2-Methyl-1-butoxy]phenyl 4-[(11-Methacryloylundec-1-yl)oxy]biphenyl-4'-carboxylate (VIIM). All methacrylate monomers VIM–VIIM were synthesized by the esterification of the corresponding alcohols VIA–VIII A, with methacryloyl chloride. An example of their synthesis is as follows. Compound VIA (1.26 g, 2.90 mmol) was dissolved in a mixture of dried THF (2 mL) and triethylamine

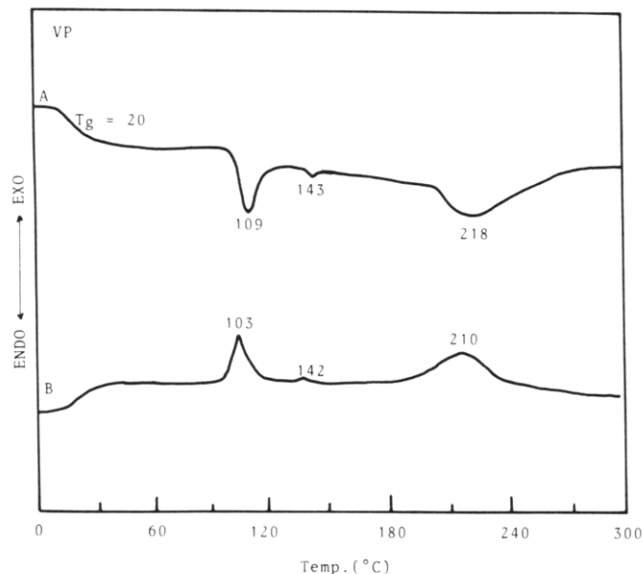


Figure 4. DSC thermogram of VP (10 °C/min): (A) second heating scan; (B) cooling scan.

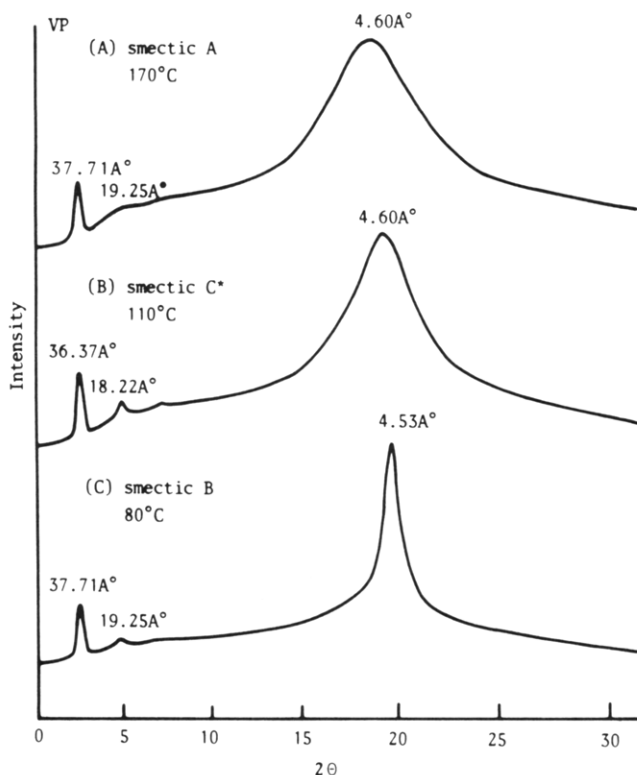


Figure 5. Temperature-dependent X-ray measurements for polymer VP at (A) 170 °C, (B) 110 °C, and (C) 80 °C.

(0.5 mL, 3.3 mmol). The resulting solution was cooled in an ice-water bath to 0 °C, and methacryloyl chloride (0.25 mL, 3.19 mmol) was added dropwise. The reaction mixture was allowed to warm slowly to room temperature and then stirred overnight. After the solution was poured into water, the precipitated product was filtered, dried under vacuum, and purified by column chromatography (silica gel, chloroform as eluent) to yield 0.8 g (55%) of white crystals. The yields, optical rotations and ^1H NMR chemical shifts of monomers VIM–VIIM are summarized in Table III.

D. Synthesis of Polysiloxanes IP–VP. The synthesis of liquid crystalline polysiloxanes is outlined in Scheme II. A general synthetic procedure is described below.

The olefin derivative, 0.8 g (10 mol % excess versus the Si–H groups present in polysiloxane), was dissolved in 80 mL of dry, freshly distilled toluene together with the proper amount of poly-

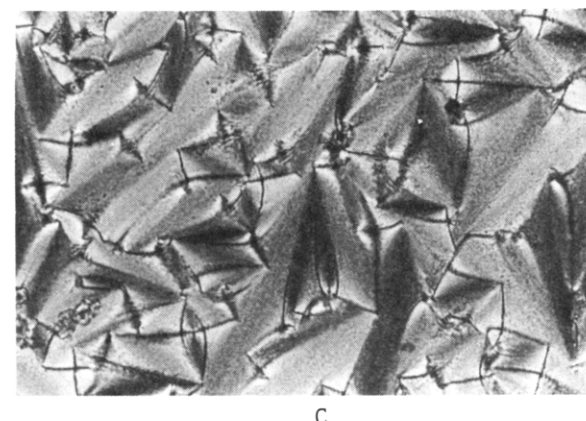
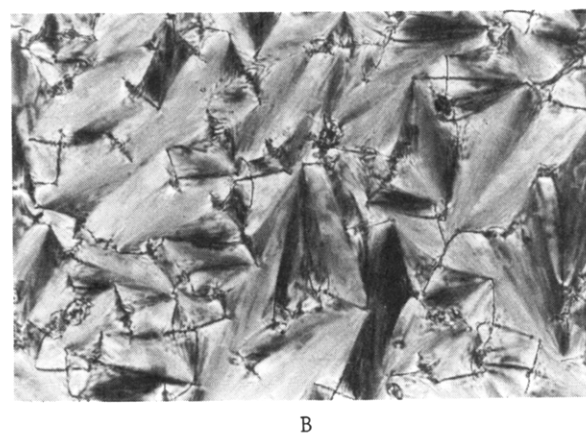
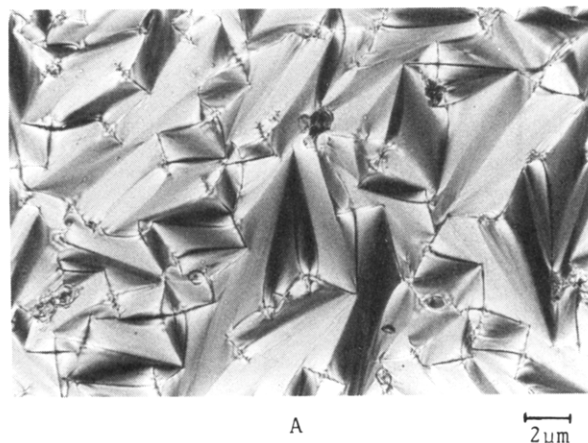


Figure 6. Optical polarizing micrographs displayed by VP: (A) S_A texture obtained after cooling to 180.9 °C; (B) S_C^* texture obtained after cooling to 134.3 °C; (C) S_B texture obtained after cooling to 106.5 °C.

(methylhydrosiloxane). The reaction mixture was heated to 110 °C under nitrogen, and 100 μg of divinyltetramethyldisiloxane platinum catalyst was then injected with a syringe as a solution in toluene (1 mg/mL). The reaction mixture was refluxed (110 °C) under nitrogen for 24 h. After this reaction time the FT-IR analysis showed that the hydrosilation reaction was complete. The polymers were separated and purified by several reprecipitations from tetrahydrofuran solution into methanol, further purified by preparative GPC, and then dried under vacuum.

E. Synthesis of Polymethacrylates VIP–VIIP. The radical polymerizations of the monomers were carried out in Schlenk tube containing the dioxane solution of the monomer (10%, wt/vol) and the initiator (AIBN, 1 wt % vs monomer) was first degassed by several freeze–pump–thaw cycles under vacuum and then filled with argon. All polymerizations were carried out at 60 °C for 15 h. After the polymerization time, the polymers

Scheme III
Synthesis of Polymethacrylates VIP-VIIIP

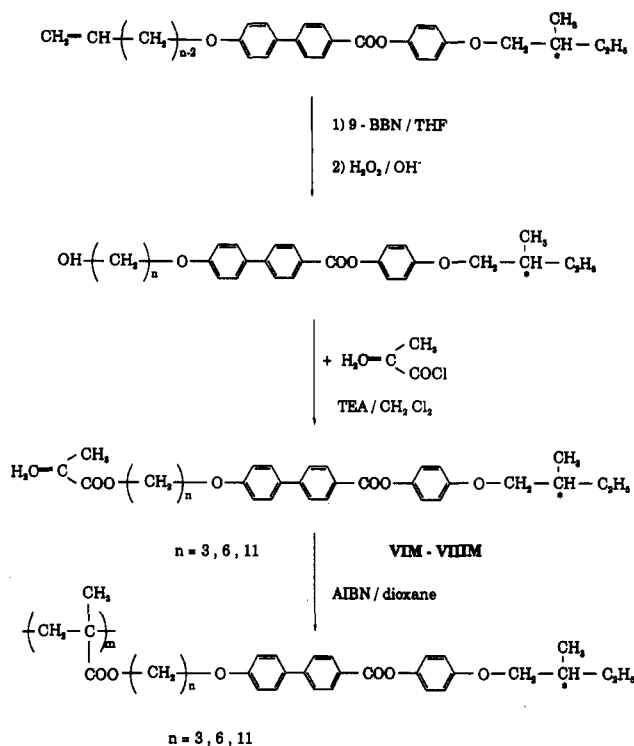


Table VI
Phase Transitions and Phase-Transition Enthalpies for Monomers VIM-VIIIM

monomer	n^a	phase transitions, °C (corresponding enthalpy changes, kcal/mol)	
		heating	cooling
VIM	3	K 81 (6.65) S_B 86 (0.58) S_A 147 (1.07) I	I 145 (1.01) S_A 85 (0.55) S_B 34 (4.08) K
VIIIM	6	K 101 (1.97) S_B 123 (0.58) S_A 149 (0.82) I	I 142 (0.97) S_A 119 (0.53) S_B 96 (2.00) K
VIIIM	11	K 88 (1.45) S_C^* 125 (-) ^b S_A 169 (0.66) I	I 165 (0.61) S_A 120 (-) ^b S_C^* 81 (0.63) S_B 65 (0.07) K

^a n according to Scheme III. ^b Enthalpy is very small.

were precipitated into methanol, filtered, and purified by reprecipitation from THF solutions into methanol. The polymerization results have been summarized in Table VII.

Results and Discussion

The synthetic route used for the preparation of 4-[(S)-2-methyl-1-butoxy]phenyl 4-(alkenyloxy)biphenyl-4'-carboxylates (IM-VM) is outlined in Scheme I. The chiral group was inserted into these mesogenic compounds starting with the commercially available (-)-2-(S)-methyl-1-butanol. This was done by a sequence of reactions which avoided its racemization. The monomers IM-VM were characterized by differential scanning calorimetry and optical polarizing microscopy. Representative DSC traces of monomers IM and VM are presented in Figure 1. Monomer IM exhibits a melting transition at 130 °C, a smectic A to cholesteric phase transition at 186 °C, and a cholesteric to isotropic phase transition at 200 °C on the heating scan (curve A). Crystallization temperature is more supercooled on the cooling scan (curve B) than the other two phase-transition temperatures. Curves C and

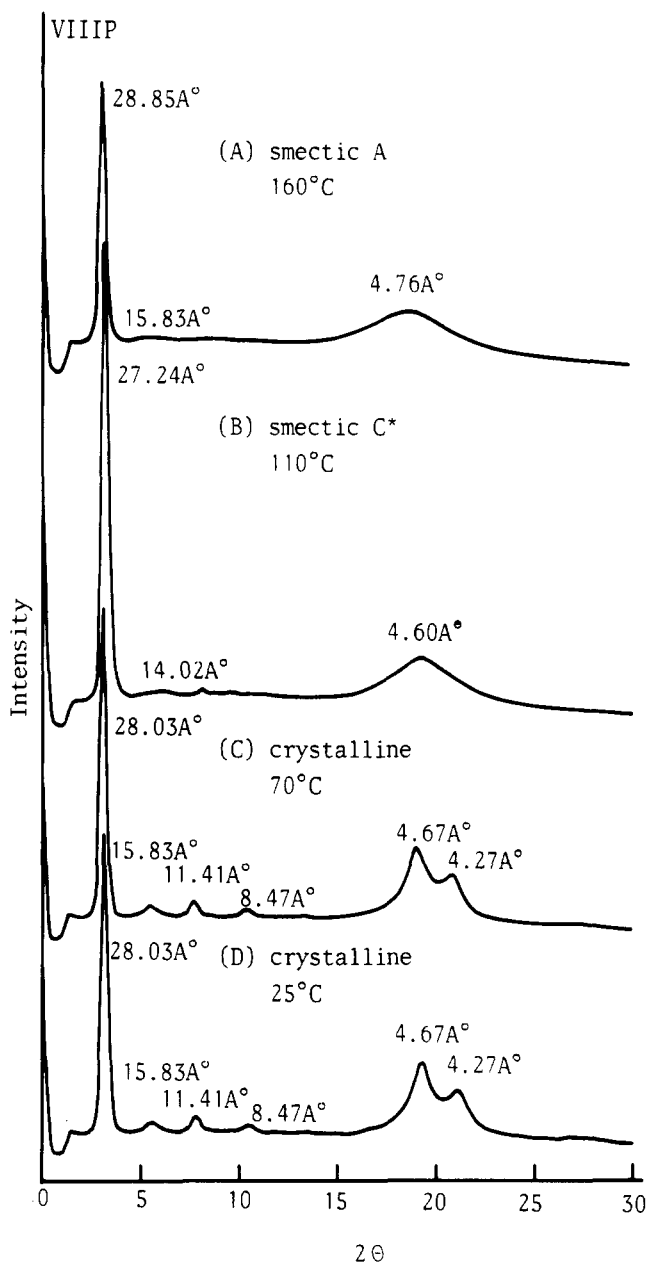


Figure 7. Temperature-dependent X-ray measurements for polymer VIIIP at (A) 160 °C, (B) 110 °C, (C) 70 °C, and (D) 25 °C.

D from Figure 1 are typical DSC traces for monomer VM. It displays smectic B, chiral smectic C, and smectic A mesophases on both heating and cooling scans. The mesophase identifications have been achieved by optical polarizing microscopic observation and X-ray diffraction measurements. The thermal transitions and thermodynamic parameters of monomers IM-VM are summarized in Table IV. As can be seen from Table IV the tendency toward chiral smectic C mesomorphism increases by increasing the length of alkenyloxy spacer.

The synthesis of polymers IP-VP is described in Scheme II. An excess amount of olefin monomers was usually used to carry the hydrosilation reaction to completion. The unreacted monomers were removed by several reprecipitations from tetrahydrofuran solution into methanol and by preparative GPC. Therefore the polymers were isolated with high purity. Table V summarizes the thermal transitions and thermodynamic parameters of the obtained polymers IP-VP. All five polymers present smectic mesomorphism. Both polymers IP and IIP show respectively an enantiotropic smectic A phase, while polymer

Table VII
Molecular Weights, Phase Transitions, and Phase-Transition Enthalpies for Polymers VIP-VIIP

polymer	n^a	\bar{M}_w	\bar{M}_n	Z	phase transitions, °C (corresponding enthalpy changes, kcal/mru ^b)
					<u>heating</u> cooling
VIP	3	22 030	17 994	1.22	G 33 S _B 84 (0.33) S _A 196 (0.97) I I 193 (0.88) S _A 81 (0.42) S _B
VIIP	6	19 889	11 814	1.68	G 31 S _B 131 (0.75) S _A 181 (1.73) I I 176 (1.70) S _A 127 (0.72) S _B
VIIP	11	20 632	15 442	1.34	G 30.5 K 101 (0.83) S _C * 132 (-) ^c S _A 197 (0.39) I I 207 (0.50) S _A 130 (-) ^c S _C * 96 (0.75) K

^a n according to Scheme III. ^b mru = mole repeating unit. ^c Enthalpy is very small.

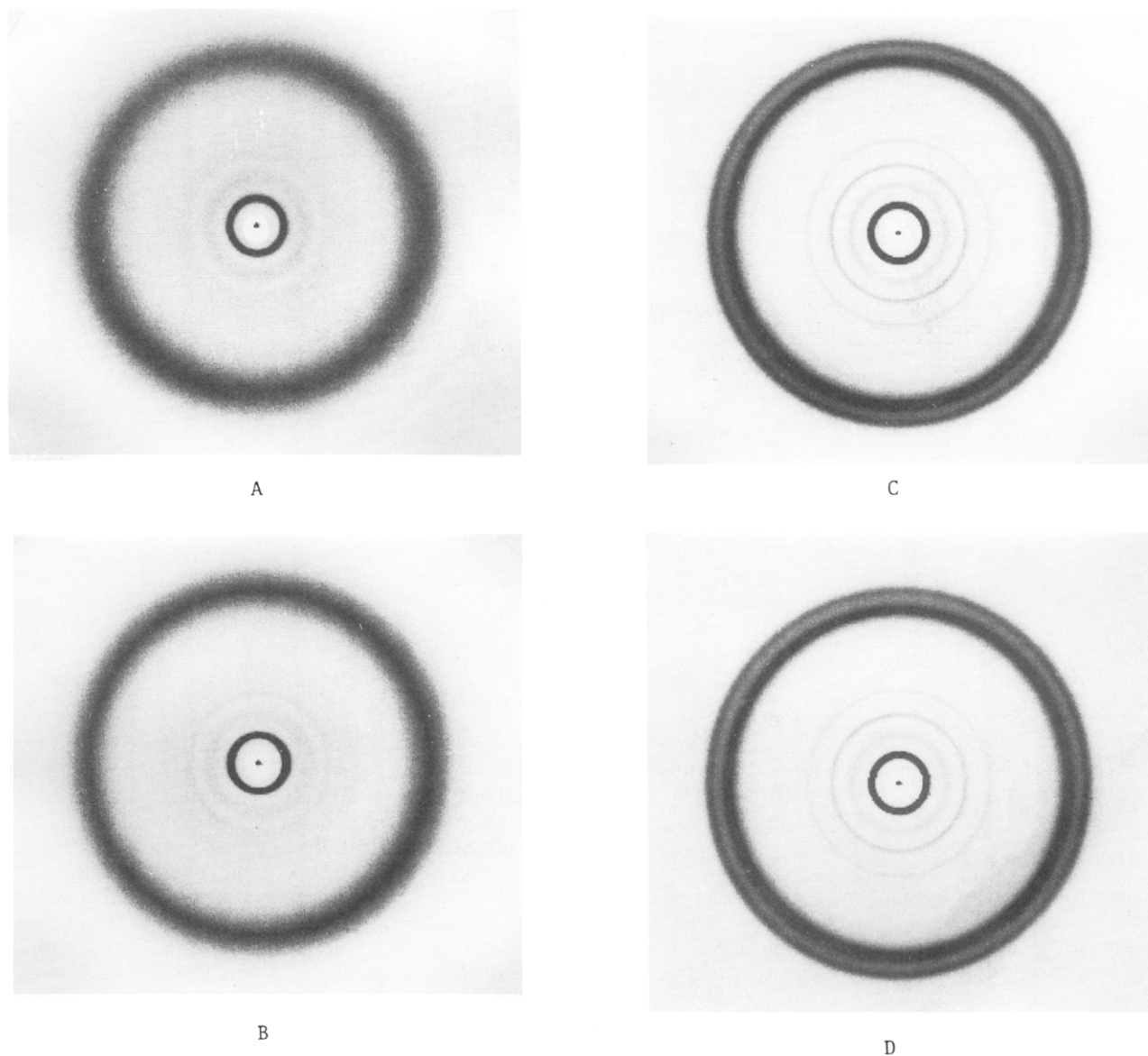


Figure 8. Wide-angle X-ray diffraction patterns for polymer VIIP obtained at (A) 160 °C, (B) 120 °C, (C) 70 °C, and (D) 25 °C.

VIIP shows enantiotropic smectic A and smectic B phases. Polymers IVP and VP are the only two polymers which reveal an enantiotropic chiral smectic C phase besides the smectic A and smectic B phases. The phase assignment was conducted by optical polarizing microscopic observation and X-ray diffraction measurements. Figure 2 presents the temperature-dependent X-ray diffraction

diagrams obtained from powder samples of IVP at 170, 120, 80, and 25 °C. A broad reflection at wide angles (associated with the lateral packings) and a sharp reflection at low angles (associated with the smectic layers) are respectively shown by all curves. Curve A presents a diffuse reflection at about 4.65 Å, which corresponds to lateral spacing of two mesogenic side groups, and a sharp

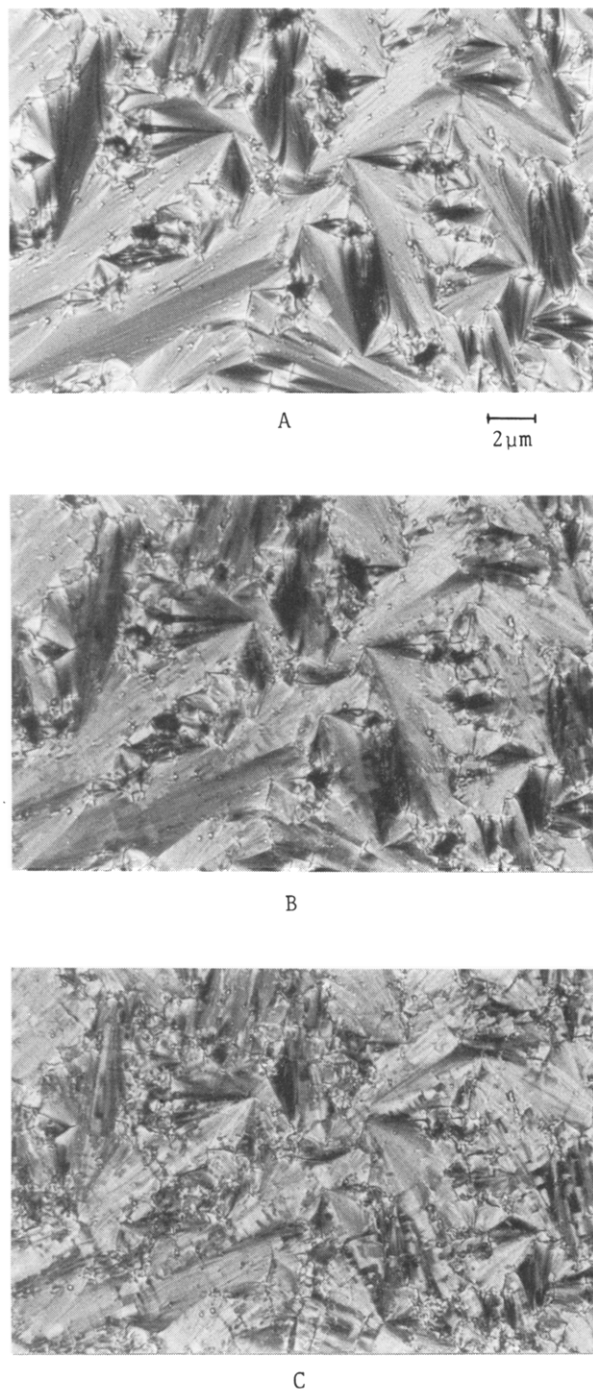


Figure 9. Optical polarizing micrographs displayed by VIIIIP: (A) S_A texture obtained after cooling to 160.9 °C; (B) S_C^* texture obtained after cooling to 127 °C; (C) crystalline texture obtained after cooling to 80 °C.

first-order reflection at 36.78 Å and a second-order reflection at 19.41 Å, which correspond to smectic layers. The optical polarizing micrograph (Figure 3A) reveals a focal-conic fan texture for polymer IVP at this temperature range. Both results are consistent with a smectic A structure. When the measuring temperature has been lowered from 170 to 120 °C, the d spacing of the first-order reflection decreases from 36.78 to 36.03 Å (curve B). This gives strong evidence for the formation of the tilted chiral smectic C phase. This result is also in agreement with the optical microscopic observation which reveals a broken fan texture (Figure 3B). When the measuring temperature has been further cooled to 80 °C, the d spacing of first-order reflection changes back to 36.78 Å and the

wide-angle reflection becomes very sharp (curve C). These results indicate the formation of a smectic B phase. Curve D which has been measured at room temperature, is eventually identical to curve C. This demonstrates that the smectic B phase has been quenched to room temperature. Figure 3C displays the smectic B texture exhibited by IVP.

Representative DSC traces for polymer VP are presented in Figure 4. A glass transition at 20 °C is displayed here, followed by a smectic B to chiral smectic C phase transition at 109 °C, a chiral smectic C to smectic A phase transition at 143 °C, and a smectic A to isotropic phase transition at 218 °C on the heating scan (curve A). The cooling scan (curve B) looks almost identical to the heating scan, except that a very small supercooling (less than 10 °C) is observed for three exothermic transitions. The temperature-dependent X-ray diffraction diagrams obtained from powder samples of VP at 170, 110, and 80 °C are presented in Figure 5. These results are very similar to those presented in Figure 2. The d spacings of first-order reflections show respectively a value of 37.71 Å at 170 °C (curve A), 36.37 Å at 110 °C (curve B), and 37.71 Å at 80 °C (curve C). These values are very close to those exhibited by polymer IVP. However, when the chemical structures of both polymers are compared, VP is five methylene units longer in its spacer. This result seems due to larger amount of overlapping of side groups in polymer VP. Figure 6 presents the typical textures exhibited by the smectic A, chiral smectic C, and smectic B phases of VP.

The synthesis of methacrylate monomers and polymers is described in Scheme III. The hydroboration of the vinyl groups of monomers IM, IVM, and VM with 9-BBN gave only the primary alcohol, which by esterification with methacryloyl chloride led to the corresponding monomers VIM–VIIM. All reaction steps were performed with retention of configuration of the chiral end groups. The thermal transitions and thermodynamic parameters of monomers VIM–VIIM are summarized in Table VI. Both monomers VIM and VIIM show enantiotropic smectic A and smectic B phases, while monomer VIIM presented enantiotropic smectic A and chiral smectic C phases and a monotropic smectic B phase.

The results of the radical polymerization of the monomers are summarized in Table VII. All polymers were purified by several precipitations until GPC measurements could not detect traces of unreacted monomers. The molecular weights of these polymers were determined by GPC using a calibration based on polystyrene standards and therefore have only a relative meaning. The thermal transitions and thermodynamic parameters of polymers VIP–VIIP have also been reported in Table VII. All three polymers show smectic mesomorphism. Both polymers VIP and VIIP, respectively, show a glass transition temperature at 33 and 31 °C and enantiotropic smectic A and smectic B phases. Polymer VIIP, which contains 11 methylene units in the spacers, presents a glass transition temperature at 30.5 °C and enantiotropic smectic A and chiral smectic C phases and a crystalline phase. Figure 7 presents the temperature-dependent X-ray diffraction diagram of polymer VIIP. Curves A and B are consistent respectively with smectic A and chiral smectic C structures. Both curves C and D show a series of small-angle reflections at 28.03, 15.83, 11.41, and 8.47 Å and two wide-angle reflections at 4.67 and 4.27 Å. These results indicate the formation of a crystalline phase. Figure 8 shows the wide-angle diffraction patterns of VIIP. Figure 9 presents the textures exhibited by VIIP. Both figures also demonstrate the formation of smectic A, chiral smectic C, and

crystalline phases. Upon comparison of the thermal transitions and corresponding enthalpy change data of polymer VIIIIP to those of polymer VP, a flexible polymer backbone can be seen here to have a tendency toward having a lower glass transition, wider mesomorphic ranges, and larger enthalpy changes. The most important tendency is that the flexible polymer backbone also leads to a wider temperature range of the chiral smectic C phase.

In conclusion, a series of new side-chain liquid crystalline polysiloxanes and polymethacrylates containing 4-[(S)-2-methyl-1-butoxy]phenyl 4-(alkyloxy)biphenyl-4'-carboxylate side groups has been prepared. All the obtained polymers have exhibited smectic mesomorphism. The tendency toward chiral smectic C mesomorphism increases by increasing the length of the alkyloxy spacers. Flexible polymer backbones enhance the decoupling of the motions of the side chain and main chain and therefore tend to give rise to a higher thermal stability of the mesophases, including the chiral smectic C phase.

Acknowledgment. The authors are grateful to the National Science Council of the Republic of China for financial support of this work (Grants NSC79-0416-E009-02 and 80-0416-E009-02).

References and Notes

- (1) Mayer, R. B.; Liebert, L.; Strzelecki, L.; Lellier, P. *J. Phys. Lett.* 1975, 36, L-69.
- (2) Clark, N. A.; Lagerwall, S. T. *Appl. Phys. Lett.* 1980, 36, 899.
- (3) Shibaev, V. P.; Kozlovsky, M. V.; Beresnev, L. A.; Blinov, L. M.; Plate, N. A. *Polym. Bull.* 1984, 12, 299.
- (4) Decobert, G.; Soyer, F.; Dubois, J. C. *Polym. Bull.* 1985, 14, 179.
- (5) Guglielminetti, J. M.; Decobert, G.; Dubois, J. C. *Polym. Bull.* 1986, 16, 411.
- (6) Decobert, G.; Dubois, J. C.; Esselin, S.; Noel, C. *Liq. Cryst.* 1986, 1, 307.
- (7) Dubois, J. C.; Decobert, G.; LeBarny, P.; Esselin, S.; Friedrich, C.; Noel, C. *Mol. Cryst. Liq. Cryst.* 1986, 137, 349.
- (8) Esselin, S.; Bosio, L.; Noel, C.; Decobert, G.; Dubois, J. C. *Liq. Cryst.* 1987, 2, 505.
- (9) Zentel, R.; Reckert, G.; Reck, B. *Liq. Cryst.* 1987, 2, 83.
- (10) Hahn, B.; Percec, V. *Macromolecules* 1987, 20, 2961.
- (11) Bualek, S.; Kapitza, H.; Meyer, J.; Schmidt, G. F.; Zentel, R. *Mol. Cryst. Liq. Cryst.* 1988, 155, 47.
- (12) Uchida, S.; Morita, K.; Miyoshi, K.; Hashimoto, K.; Kawasaki, K. *Mol. Cryst. Liq. Cryst.* 1988, 155, 93.
- (13) Esselin, S.; Noel, C.; Decobert, G.; Dubois, J. C. *Mol. Cryst. Liq. Cryst.* 1988, 155, 371.
- (14) Kapitza, H.; Zentel, R. *Makromol. Chem.* 1988, 189, 1793.
- (15) Zentel, R. *Liq. Cryst.* 1988, 3, 531.
- (16) Zentel, R.; Reckert, G.; Bualek, S.; Kapitza, H. *Makromol. Chem.* 1989, 190, 2869.
- (17) Vallerien, S. U.; Zentel, R.; Kremer, F.; Laptiza, H.; Fischer, E. W. *Makromol. Chem., Rapid Commun.* 1989, 10, 33.
- (18) Scherowsky, G.; Schliwa, A.; Springer, J.; Kuhnpast, K.; Trapp, W. *Liq. Cryst.* 1989, 5, 1281.
- (19) Shibaev, V. P.; Kozlovsky, M. V.; Plate, N. A. *Liq. Cryst.* 1990, 8, 1281.
- (20) Dumon, M.; Nguyen, H. T.; Mauzac, M.; Destrade, C.; Achard, M. F.; Gasparoux, H. *Macromolecules* 1990, 23, 355.
- (21) Vallerien, S. U.; Kremer, F.; Fischer, E. W. *Makromol. Chem., Rapid Commun.* 1990, 11, 593.
- (22) Vallerien, S. U.; Kremker, F.; Kapitza, H.; Zentel, R.; Fischer, E. W. *Ferroelectrics* 1990, 109, 273.
- (23) Brand, H. R.; Pleiner, H. *Makromol. Chem., Rapid Commun.* 1990, 11, 607.
- (24) Endo, H.; Hachiya, S.; Uchida, S.; Hashimoto, K.; Kawasaki, K. *Liq. Cryst.* 1991, 9, 635.
- (25) Kapitza, H.; Zentel, R. *Makromol. Chem.* 1991, 192, 1859.
- (26) Bomelburg, J.; Heppke, G.; Hollidt, J. *Makromol. Chem., Rapid Commun.* 1991, 12, 483.
- (27) LeBarny, P.; Dubois, J. C. In *Side Chain Liquid Crystal Polymers*; McArdle, C. B., Eds.; Blackie: Glasgow and London, 1989; p 130.
- (28) Percec, V.; Hahn, B. *J. Polym. Sci., Polym. Chem. Ed.* 1989, 27, 2367.
- (29) Percec, V.; Hsu, C. S.; Tomazos, D. *J. Polym. Sci., Polym. Chem. Ed.* 1988, 26, 2047.